Cohen, R. E., & Ballou, C. E. (1980) *Biochemistry 19*, 4345–4358.
Cook, W. J., & Bugg, C. E. (1975) *Biochim. Biophys. Acta 389*, 428–435.
Dabrowski, J., Hanfland, P., & Egge, H. (1980) *Biochemistry 19*, 5652–5658.
Doddrell, D., Glushko, V., & Allerhand, A. (1972) *J. Chem. Phys. 56*, 3683–3689.
Dorland, L., Schut, B. L., Vliegenthart, J. F. G., Strecker, G., Fournet, B., Spik, G., & Montreuil, J. (1977) *Eur. J. Biochem. 73*, 93–97.
Fries, D. C., Rao, S. T., & Sundaral, M. (1971) *Acta Crystallogr., Sect. B B27*, 994–1005.
Goldstein, I. J., & Hayes, C. E. (1978) *Adv. Carbohydr. Chem. Biochem. 35*, 127–340.
Harpaz, N., & Schachter, H. (1980) *J. Biol. Chem. 255*, 4894–4902.
Hayes, M. L., Serianni, A. S., & Barker, R. (1982) *Carbohydr. Res. 100*, 87–101.
Hughes, R. C., & Sharon, N. (1978) *Nature (London) 274*, 637–638.
Jeffrey, G. A., McMullian, R. K., & Takagi, S. (1977) *Acta Crystallogr., Sect. B B33*, 728–737.
Lemieux, R. U., Bock, K., Delbaere, L. T. J., Koto, S., & Rao, V. S. (1980) *Can. J. Chem. 58*, 631–653.
Mo, F. (1979) *Acta Chem. Scand., Ser. A A33*, 207–218.
Narasimhan, S. (1982) *J. Biol. Chem. 257*, 10235–10242.
Noggle, J. H., & Schirmer, R. E. (1971) *The Nuclear Overhauser Effect*, Academic Press, New York.
Ogawa, T., & Yamamoto, H. (1982) *Carbohydr. Res. 104*, 271–283.
Potenzone, R., & Hopfinger, A. J. (1975) *Carbohydr. Res. 40*, 323–335.
Rees, D. A., & Skerett, R. J. (1970) *J. Chem. Soc. B*, 189–193.
Schachter, S., & Roseman, S. (1980) in *The Biochemistry of Glycoprotein and Proteoglycans* (Lennarz, W. J., Ed.) pp 85–160, Plenum Press, New York.
Sykes, B. D., Hull, W. E., & Snyder, G. H. (1978) *Biophys. J. 21*, 137–146.
Thogersen, H., Lemieux, R. U., Bock, K., & Meyer, B. (1982) *Can. J. Chem. 60*, 44–57.
Tvaroska, I., Perez, S., & Marchessault, R. H. (1978) *Carbohydr. Res. 61*, 97–106.
van Halbeek, H., Dorland, L., Veldink, G. A., Vliegenthart, J. F. G., Strecker, G., Michalski, J.-C., Montreuil, J., & Hull, W. E. (1980) *FEBS Lett. 121*, 71–77.
Warin, V., Baert, F., Fouret, R., Strecker, G., Spik, G., Fournet, B., & Montreuil, J. (1979) *Carbohydr. Res. 76*, 11–22.
Winnik, F. M., Brisson, J.-R., Carver, J. P., & Krepinsky, J. J. (1982a) *Carbohydr. Res. 103*, 15–28.
Winnik, F. M., Carver, J. P., & Krepinsky, J. J. (1982b) *J. Org. Chem. 47*, 2701–2707.

Solution Conformation of Asparagine-Linked Oligosaccharides: $\alpha(1-6)$-Linked Moiety†

Jean-Robert Brisson and Jeremy P. Carver*

ABSTRACT: The solution conformation is presented for representatives of each of the major classes of asparaginyl oligosaccharides. In this report the conformation of the $\alpha(1-6)$-linked moiety is described. The conformational properties of these glycopeptides were determined by high-resolution ^1H nuclear magnetic resonance in conjunction with potential energy calculations. The NMR parameters that were used in this analysis were chemical shifts and nuclear Overhauser enhancements. Potential energy calculations were used to evaluate the preferred conformers available for the different linkages in glycopeptides and to draw conclusions about the behavior in solution of these molecules. For all classes, identical conformations were found for the 6-arm *except* for the torsional angle, ω, about the C5–C6 bond of the $\alpha 1-6$ linkage. For high mannose and hybrid structures ω was found to be −60°, for bisected biantennary complex structures ω was 180°, and for complex biantennary structures averaging between −60° and 180° occurs.

In the preceding paper (Brisson & Carver, 1983a), the solution conformations of $\alpha(1-3)$-, $\alpha(1-2)$-, $\beta(1-2)$-, and $\beta(1-4)$-linked units of asparagine-linked oligosaccharides were examined. For all the major classes of glycopeptides, it was found that the conformation of any particular linkage was essentially the same from one to the other, although the conformations of different linkages were quite dissimilar. The inhibitory effect of the bisecting GlcNAc for certain enzymes involved in the biosynthetic pathway of glycopeptides (Narasimhan, 1982) was also explained. The position of the bisecting GlcNAc in the structure was found to be such that its ring covered a wide area on the surface of GlcNAc$\beta 1-2$Man$\alpha 1-3$Man$\beta 1-$ unit, thus sterically hindering those enzymes from binding to this determinant.

In this paper the orientation of the $\alpha(1-6)$-linked moiety in the different classes of N-linked oligosaccharides is described. In contrast to the invariance of the $\alpha 1-3$ linkage, major differences in the torsional angle about the C5–C6 bond of the $\alpha 1-6$ linkages are found.

Experimental Procedures

The experimental methods and methods of calculation are described in detail in the preceding paper (Brisson & Carver,

† From the Departments of Medical Genetics and Medical Biophysics, University of Toronto, Toronto, Ontario, Canada M5S 1A8. *Received February 24, 1983.* This research was supported by grants from the Medical Research Council of Canada (MT-3732 and MA-6499) and a studentship (J.-R.B.).

0006-2960/83/0422-3680$01.50/0

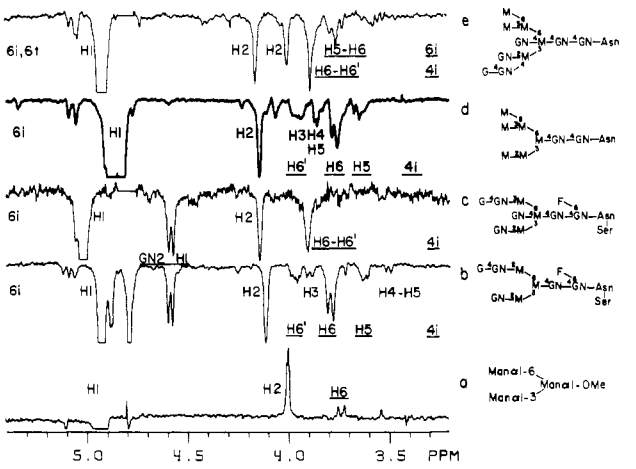

FIGURE 1: NOE spectra for saturation of the Manα1–6 H1 resonance in (a) Manα1–6(Manα1–3)Manα1–OMe, (b) GGN, (c) GGN(GN), (d) D3 (6i), and (e) A3 (6i and 6t).

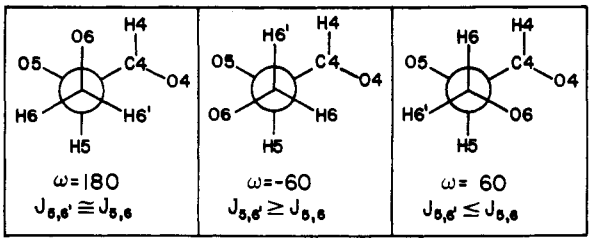

FIGURE 2: Rotamers about the C5–C6 bond for a hydroxymethyl group. ω = (O6, C6, C5, H5). Due to an unfavorable interaction between O6 and O4, the ω = 180° and ω = −60° are the preferred rotamers in solution. Hence, for the coupling constants in solution, $J_{5,6'}$ is thus greater or equal to $J_{5,6}$ because these are weighted averages of the coupling constants for each rotamer.

1983a). The long-range shielding from the carbonyl group of GlcNAc was estimated by using the equations of ApSimon & Beierbeck (1971). The calculation included magnetic anisotropic and electrostatic shielding effects on the chemical shifts of nearby protons.

Results and Discussion

The structures of the asparaginyl oligosaccharides and the nomenclature used to designate them are given in the preceding paper (Brisson & Carver, 1983a).

Orientation of the 6-Arm in Complex Structures. On saturation of 6i H1 in GGN, interresidue NOE's were observed for 4i H6, H6′, and H5 (Figure 1b). The major NOE appeared on the H6 signal just as in the synthetic methyl mannotrioside (Figure 1a). From NOE and ^{13}C studies on the latter compound (Brisson & Carver, 1983b), conformational averaging was found to be restricted to ϕ values ranging from −60° to −30° and to ψ values ranging from 150° to 200°, while ω could adopt two preferred orientations (Figure 2). The larger relative NOE on H6, the sign of the NOE, and the appearance of NOE's on the H5 and H6′ signals on saturation of 6i H1 in GGN are all attributable to the longer correlation times of the protons involved.

From an examination of line fits for the multiplet patterns of the NOE signals of 4i (Figure 3a), $J_{5,6}$ and $J_{5,6'}$ were found to be 1 ± 1 and 5.5 ± 0.5 Hz, respectively. These coupling constants reflect the population distribution of the rotamers about the C5–C6 bond for hydroxymethyl groups (Figure 2). Since, the rotamer ω = 60° is unfavored (Marchessault & Perez, 1979; De Bruyn & Anteunis, 1976; Gagnaire et al., 1973), the observed coupling are the weighted average of the couplings for the two rotamers ω = 180° and ω = −60°.

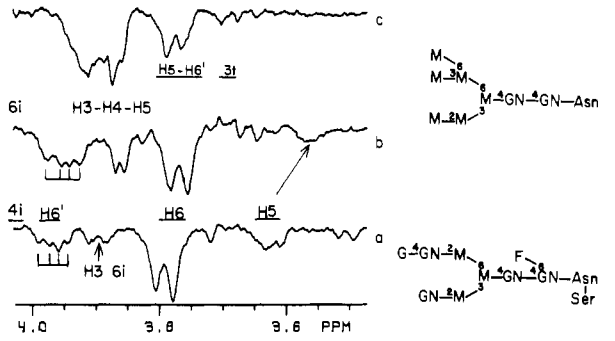

FIGURE 3: Estimation of $J_{5,6'}$ at the Manα1–6 linkage from NOE spectra. NOE spectra for saturation of 6i H1 in (a) GGN and (b) in D3. (c) NOE spectrum for saturation of 6i H2 demonstrating the possibility of overlap of NOE's between the 4i H6 and 6i H3–H4–H5 complex signal in the NOE spectrum on saturation of 6i H1 (b).

Therefore, $J_{5,6}$ should always have a small value, since for both favorable rotamers, the vicinal coupling between H5 and H6 will be small (1–2 Hz). In contrast, $J_{5,6'}$ will vary considerably depending on the population distribution of the rotamers. For the bisecting GlcNAc a unique rotamer with ω = −60° was found and $J_{5,6'}$ had a value of 8 Hz (Brisson & Carver, 1983a). Thus, $J_{5,6'}$ will vary from 1–2 to 8 Hz depending on the population distribution of the rotamers. Since for GGN a value of 5.5 ± 0.5 Hz is observed, both rotamers are equally probable in solution. Thus, the substitutions on the mannotriose unit do not affect the conformational mobility about the C5–C6 bond.

The observed relative NOE for the 4i H6 resonance, on saturation of 6i H1, is much larger than the computed one for any energetically favorable conformations (0.5 vs. 1.3 ± 0.5) (Table I). This discrepancy can be corrected by decreasing the correlation time for 6i H2 with respect to 4i H6, since this results in a smaller predicted NOE on the 6i H2 and therefore a larger predicted relative NOE. Differences in correlation times for different atoms arise either from anisotropic tumbling or internal motion about the glycosidic bonds at rates similar to the tumbling rate of the molecule. In this case, the difference between the computed and observed relative NOE's for 4i H6 probably arises from conformational averaging between the two stable rotamers (ω = 180° and ω = −60°) about the 4i C5–C6 bond.

Orientation of the 6-Arm in Bisected Complex Structures. Large chemical shift differences are observed between GGN and GGN(GN) (Table II). The cause of the chemical shift perturbations on the 3-arm was previously determined to arise simply from the proximity of the bis GN in the structure since no major conformational changes on the 3-arm were detected from NOE experiments (Brisson & Carver, 1983a). In contrast, the chemical shift differences of protons located on the 6-arm are interpreted as arising from major conformational changes about the Manα1–6 linkage in complex and bisected complex structures.

On saturation of 6i H1 in GGN(GN), an NOE is observed on 4i H6–H6′ (Figures 1c and 4b). The vicinal coupling constants with H5, which are indicative of the orientation of the 6-arm, could not be extracted from the line shape due to strong coupling (Figure 4b). However, the 4i H5 resonance was located by spin tickling of the isolated 4i H4 resonance (Figure 4d) and also observed in the NOE spectrum for saturation of 4i H1 (Figure 4c). The other resonances that appear in the NOE spectrum (Figure 4c) are due to the simultaneous irradiation of the core GN H1 resonance. The broad resonance which occurs downfield of the 4i H5 resonance arises from the core GN H5. The latter resonance was

Table I: Nuclear Overhauser Enhancements[a]

		relative NOE				
		GGN			GGN(GN)	
saturated signal		obsd	calcd		obsd	calcd
6i H1	6i H2	[0.11]	1.0	6i H2	[0.10]	1.0
	6i H3	0.6	0.3			
	4i H6	1.3	0.5	4i H6-H6′	1.0	1.2
	4i H6′	0.5	0.1			
	4i H5	0.5	0.1			
	GN2 H1	0.9	1.2	GN2 H1	1.5	1.2

		relative NOE				
		D3			A3	
saturated signal		obsd	calcd		obsd	calcd
6i H1	6i H2	[0.07]	1.0	6i H2	[0.08]	1.0
	6i H3-H4-H5	0.4	0.4			
	4i H6	1.3	0.8	4i H6-H6′	1.7	1.3
	4i H6′	0.4	0.3			
core GN CH_3	core GN H1	0.2	0.1			
	core GN H2-H3-H4	1.0[b]	[0.03]			
	Asn GN H6′					
	Asn GN H6	0.4	0.8			
	Asn GN H5	0.2	0.2			
	3t H1	0.3	0.4			
	3t H2	0.4	0.2			
	4i H2	0.1	0.0			

[a] The numbers enclosed in brackets are the absolute NOE used to calculate the relative NOE's. [b] Because of the difficulties in quantitating small absolute NOE's, the observed values are expressed relative to the NOE found for the complex signal from the core GN H2-H3-H4 and the Asn GN H6′. The absolute NOE calculated for this complex was 0.03.

Table II: Chemical Shift Perturbations Due to the Bisecting GlcNAc

	H1	H2	H3	H4	H5	H6	H6′	NH[c]
complex type[a] residue								
4i	−0.081	−0.080	0.10	0.31	−0.08	0.11	−0.06	
6i	0.087	0.028	−0.06					
6GN2	−0.003	−0.003	−0.14	0.00	−0.11			−0.12
core GN	−0.008	0.04						−0.04
Fuc	0.008	0.00		0.05	0.01	0.01		
hybrid type[b] residue								
4i	−0.038	−0.059	0.11	0.11	0.00	0.12	−0.07	
6i	0.048	0.019	0.00					
3t	−0.046	0.000	−0.01					
6t	0.025	0.021	0.02					
core GN	−0.012	−0.01	−0.01					

[a] Chemical shifts of GGN(GN) minus those of GGN. [b] Chemical shifts of C3B minus those of GNM_5. [c] Unpublished results.

identified as such since it had the same chemical shift and the same shape as the core GN H5 resonance observed in the NOE spectrum for saturation of the isolated core GN H1 resonance in GGN. The broad doublet appearance for the H5 signal could only be reproduced adequately with $J_{5,6} = J_{5,6'} = 2$ Hz and $J_{6,6'} = -11.5$ Hz (Figure 4e), indicating that $\omega = 180°$ at the Manα1–6 linkage. The H6 and H6′ strongly coupled signal (Figure 4b) was also reproduced accordingly (Figure 4e). Thus, the presence of bis GN in GGN(GN) results in the restriction of the orientation of the 6-arm to only one conformer ($\omega = 180°$).

This restriction in the orientation of the 6-arm in GGN(GN) provides an explanation for all the differences in chemical shift observed between the GGN and GGN(GN) (Table II). The large downfield shift (0.31 ppm) of the 4i H4, between GGN and GGN(GN), is attributed to the orientation of the hydroxymethyl oxygen which is now adjacent to the 4i H4 (Figure 2) and thus deshields the signal of the former. The perturbations observed on resonances of the 6GN2 and the core GN residues in GGN(GN) arise from the close proximity of these two residues, since, with $\omega = 180°$ at the α1–6 linkage, the 6-arm is folded backward toward the core. Alterations in chemical shifts were observed on the 6GN2 H3, H5 resonances (assigned from the NOE spectrum for saturation of 6GN2 H1) and on the 6GN2 NH resonance. The Fuc H4 resonance (assigned from the NOE spectrum for saturation of the Fuc methyl resonance) was also found to be significantly different in GGN and GGN(GN) (Table II).

The above results were also consistent with the minimum energy conformer with $\omega = 180°$ at the Manα1–6 linkage. Potential energy calculations were performed for the 6-arm of GGN(GN), keeping the bis GN and the 6GN2 angles fixed, as previously determined by NOE experiments (Brisson & Carver, 1983a). The Galβ1–4 linkage conformation was taken to be the same as in the solid state (Longchambon et al., 1981). The Fucα1–6 orientation was determined by choosing a minimum in potential energy such that its orientation was similar to the one in the crystal structure of a complex type glycopeptide (Deisenhofer, 1981). The linkage conformations for the Manα1–6, Manβ1–4, and core GlcNAcβ1–4 linkages were then varied in steps of 20° over a range where no steric contacts occur for the disaccharide units. The resulting

Table III: Linkage Conformations: (ϕ, ψ) (deg, deg) for Asn-Linked Oligosaccharides

residue	6i ω	high mannose	bisected hybrid	complex	bisected complex
Manα1-6	180	(−40, 200)	(−40, 140)	(−60, 120)	(−60, 120)
	−60	(−60, 160)	(−60, 160)	(−60, 180)	(−60, 180)
GlcNAcβ1-2				(40, 30)	(40, 30)
Galβ1-4				(30, −20)	(30, −20)
Manα1-3		(−50, −10)	(−50, −10)		
Manβ1-4	180	(60, −20)	(60, −10)	(50, −10)	(50, −10)
	−60	(50, 0)	(50, 0)	(30, −50)	(30, −50)
core GN	180			(30, −50)	(30, −50)
	−60			(50, −10)	(50, −10)
Fucα1-6	180			(60, 150)	(60, 150)[b]
	−60			(60, 180)	(60, 180)
bis GN			(60, 10)		(60, 10)
relative energy[a]	180	0.8	0.4	0	0
	−60	0	0	4	5

[a] In kilocalories per mole. [b] $\omega = 180°$.

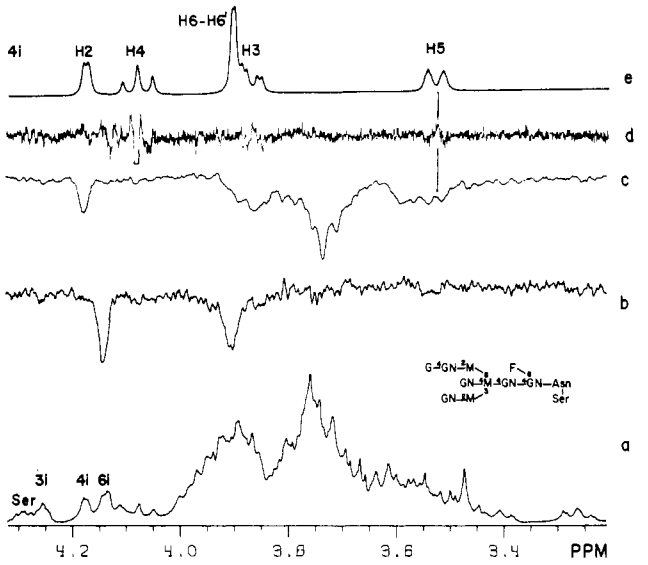

FIGURE 4: Coupling constants and chemical shifts of the Manβ1−4 residue in GGN(GN). (a) Normal spectrum of GGN(GN); (b) NOE spectrum for saturation of 6i H1 showing the detection of the strongly coupled H6−H6′ signal (3.90 ppm); (c) NOE spectrum for the simultaneous saturations of 4i H1 and the core GN H1 resonances (most of the 4i and core GN enhancements overlap, except for the H5 resonances (3.53 ppm and 3.6 ppm, respectively)]; (d) spin tickling of 4i H4 (4.077 ppm) to detect the 4i H3 resonance (3.867 ppm) and the 4i H5 resonance (3.53 ppm); (e) spectrum simulation with $J_{2,3}$ = 3.2, $J_{3,4}$ = 9.8 Hz, $J_{4,5}$ = 10.2, $J_{5,6} = J_{5,6'}$ = 2 and $J_{6,6'}$ = −11.5 Hz. All coupling constants are in hertz.

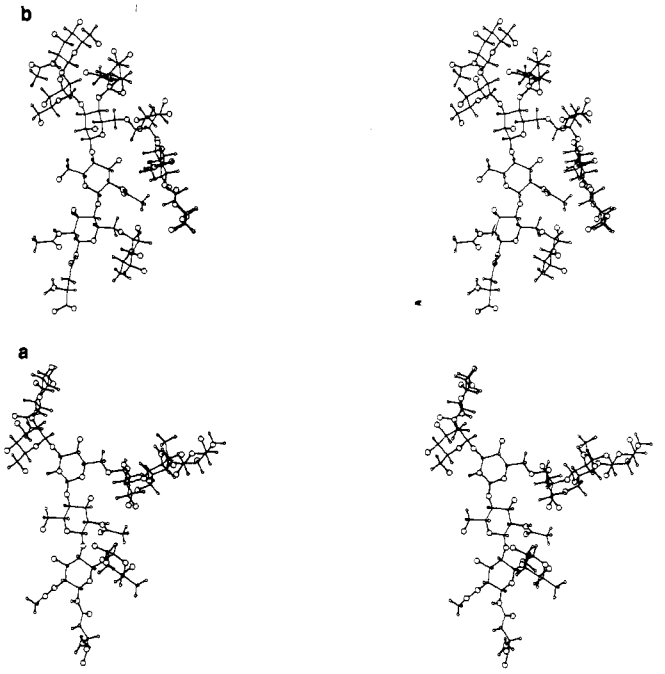

FIGURE 5: Stereo diagrams of complex structures: (a) GGN with ω = −60° at the Manα1−6 linkage; (b) GGN(GN) with ω = 180° at the Manα1−6 linkage. The large spheres are oxygen atoms, and the smaller ones are hydrogen atoms. The H atoms of hydroxyl groups have been omitted.

minimum energy conformer is given in Table III. Smaller increments for the linkage conformations near the minimum energy conformer in Table III did not significantly decrease (0.5 kcal/mol) the potential energy.

For the minimum energy conformer, H3 and H5 of 6GN2 are proximal to the acetyl group of the core GN (3–6 Å from the carbonyl oxygen). This proximity is the probable cause for the upfield shifts (as compared to GGN) observed for these resonances (Table II). By use of the theory of ApSimon & Beierbeck (1971) to estimate the shielding effect of the carbonyl group, shifts of 0.12, 0.04, and −0.38 were predicted for the H3, H5, and NH resonances. Considering that this theory was adapted to fit the shielding of keto groups on methyl groups and that effects from the methyl group are neglected, the predicted shifts serve to indicate that these protons are in a region of high magnetic field anisotropy, in agreement with the chemical shift perturbations noted on these resonances (Table II).

The Fuc H4 resonance was also appreciably different in GGN(GN) and GGN (Table II). As can be observed in the stereo diagram for GGN(GN) (Figure 5b), H4 of the Fuc residue is facing toward the Gal residue. However, the precise origin of the interaction between Gal and Fuc is not known at the present. If Fuc is oriented in the other direction about the C5–C6 bond of its α1−6 linkage (ω = −60°), the H4 is not proximal to the Gal residue and the origin of the Fuc H4 chemical shift perturbation cannot be explained.

The hypothesis that the 6-arm in bisected complex structures is folded back toward the core thus explains all the major chemical shift perturbations observed when bis GN is introduced into a complex structure. From potential calculations, the minimum energy conformer for ω = 180° was found to be favored by 5 kcal/mol over the minimum energy conformer for ω = −60°. This is in accord with the experimental observations. However, the same preference is predicted for complex structures, in sharp contrast to the experimental observations which suggest equal distributions for the rotamers ω = 180° and ω = −60°. Hence, although potential energy calculations are useful to find minima in the conformational

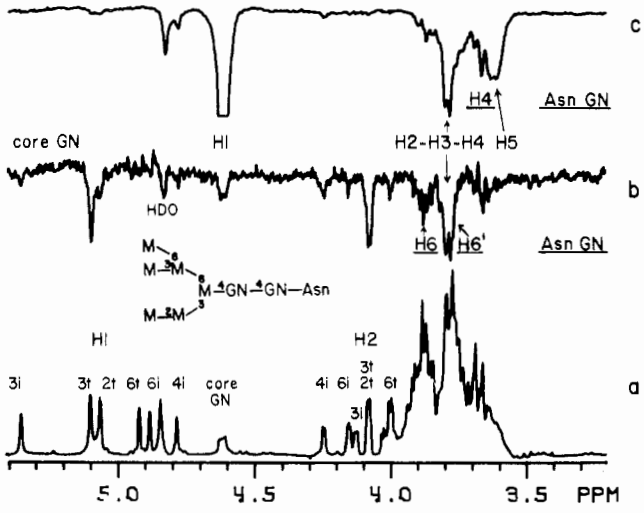

FIGURE 6: NOE between the core GN methyl resonance and the H1 and H2 resonances of the 6-arm Manα1–3 residue in a high mannose structure. (a) Normal spectrum of D3; (b) NOE spectrum for saturation of the core GN methyl resonance (2.059 ppm); (c) NOE spectrum for saturation of the core GN H1 resonance.

energy space, the population distribution among these conformers does not appear to be well predicted. Thus, other factors, which are not included in these calculations, such as solvent interactions must significantly alter the distribution of conformers in solution.

Orientation of the 6-Arm in High Mannose Structures. For D3 two observations suggest that the 6-arm is folded back toward the core with the 3t residue close to the core GN: (i) the presence of chemical shift perturbations on 3t when the core GN is present and (ii) the existence of an NOE between the CH_3 of the core GN and the H1 and H2 of 3t. In structures which contain the unit Manα1–3Manα1–6Manβ1–4GlcNAc(α,β), the 3t H1 resonance appears as two separate resonances, 0.06 ppm apart. It has been suggested that this effect arises from the different anomeric configuration at the reducing GlcNAc (Carver et al., 1981). When the core GN methyl (2.057 ppm) is saturated, interresidue enhancements ($\sim$0.01) are observed on 3t H1 and 3t H2 (Figure 6b). The other enhancements observed in this experiment are ascribed to intraresidue NOE's with the ring protons of the core GlcNAc since, in the NOE pattern for saturation of the core GN H1 resonance (Figure 6c), similar enhancements were observed. Other resonances were assigned to Asn GN on the basis that their signals were predicted from the computed NOE's (Table I).

The above effects can only arise from the close proximity of the 3t residue to the core GlcNAc. In order to attempt a more precise orientation of the 6-arm with respect to the core GN, the nonbonded and electrostatic potential energy for the structure Manα1–3Manα1–6Manβ1–4GlcNAcβ was calculated by varying, in steps of 10°, all the torsion angles about the three linkages while keeping ω fixed at either 180° or –60°. The range of angles considered covered the region of torsion angles which were energetically favorable for the individual linkages. For ω = –60° a minimum in potential energy occurred which favored the formation of a hydrogen bond between the GlcNAc carbonyl oxygen and the terminal Manα1–3 O2-H (see the stereo diagram in Figure 7). This orientation did not require any change from the linkage conformations determined in oligomannosides for the Manα1–3 and Manα1–6 linkages (Brisson & Carver, 1982b). The resulting linkage conformation of the Manβ1–4GlcNAc linkage was the same as in the solid state (Warin et al., 1979). The

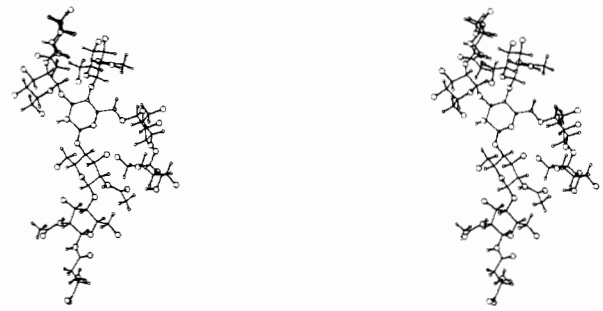

FIGURE 7: Stereo diagram showing the hydrogen-bonded structure between the core GN carbonyl oxygen and O2-H of the terminal Manα1–3 residue on the 6-arm in a bisected hybrid structure (C3B). The 6t residue has been omitted. Except for 3t O2-H, the H atoms of hydroxyl groups are not shown.

potential energy calculations, which did not include a hydrogen-bonding energy term, predicted that the rotamer for ω = 180° should be equally probable to the one for ω = –60°. However, with the inclusion of the favorable hydrogen bond between the core GN carbonyl oxygen and the 3t O2-H, the ω = –60° rotamer should be preferred.

The interresidue NOE between the methyl group of the core GN and the 3t H1 and H2 is consistent with the hydrogen-bonded conformer (ω = –60°), since the computed NOE's were comparable to the observed one (Table I). Although the error associated with the measurements are large (50–100%), the observation of these NOE's requires the 3t H1 and 3t H2 to be within 5 Å of the methyl group. Considering the large number of degrees of freedom available to the residues between 3t and the core GN, conformational variability about any of the bonds would nullify these interresidue NOE's. Therefore, the conformation with the 6-arm folded back toward the core (ω = –60°) must be relatively stable. Also, the differences between the observed and computed NOE's in D3 (Table I) were much less than those in GGN, suggesting that conformational variability about the internal Manα1–6 bond in D3 is not as pronounced as in GGN.

The unique value of ω for the internal Manα1–6 bond in D3 is consistent with the magnitude of $J_{5,6'}$, measured from the line shape of the 4i H6′ resonance in the NOE spectrum on saturation of 6i H1 (Figures 1d and 3b). The upfield doublet of the H6′ multiplet had a spacing of 6 Hz and the lowfield one a spacing of 8 Hz. The uneven spacing probably arises from the obstruction of the highfield part of the 4i H6′ multiplet by the intraresidue NOE on the 6i H3–H4–H5 complex signal (Figure 3c). The observation that $J_{5,6'}$ for D3 is larger than for GGN supports the conclusion that a single rotamer with ω = –60° is preferred in the former.

The postulate that the 6-arm is folded back toward the core also explains a number of long-range interactions between the 3t and core GN which have been identified through the observation of chemical shift perturbations. For example, in the methyl mannotetraoside

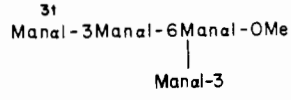

where the core GN is not present, the 3t H1 resonates at 5.154 ppm (Winnik et al., 1982), while in E3, the 3t H1 resonates at 5.092 ppm. Hence, in the latter, the H1 resonance is shielded by –0.062 ppm compared to the similar resonance in the mannotetraoside. The 3t H2 resonances in both compounds have similar chemical shifts (4.069 vs. 4.066 ppm). Reciprocal perturbations on the core GN are observed by

comparing chemical shifts between the compound Manα1–6Manβ1–4GlcNAcβ1–4GlcNAc–Asn and E3 (van Halbeek et al., 1980): the core GN H1 resonance (4.618 vs. 4.601 ppm) and the core GN CH_3 resonances (2.076 vs. 2.060 ppm) are significantly different. The core GN H2–H3 relative chemical shift is also significantly different (>0.01 ppm) between these two compounds, as judged by the appearance of virtual coupling on the core GN H1 when a terminal Manα1–3 residue is present on the internal Manα1–6 residue (Brisson & Carver, 1982). Such widespread perturbations over most of the proton resonances of the core GN can be explained by the proximity of the 3t residue.

The perturbations on the 3t H1 resonances are also compatible with the long-range shielding effect of the carbonyl group on the H1 and H2 signals of the 3t resonances estimated by using the theory of ApSimon & Beierbeck (1971). A shielding of –0.22 ppm and a deshielding of 0.03 ppm were predicted on the 3t H1 and H2 resonances for the conformer with $\omega = -60°$. As described before for GGN, these values serve to indicate that 3t H1 and 3t H2 are in a region of high magnetic field anisotropy. Thus, a change of ±10° in any of the torsion angles between the core GN and 3t leads to large changes (± 0.2 ppm) in the shielding on the 3t H1 and H2. Hence, the α,β effect in the oligosaccharides containing Manα1–3Manα1–6Manβ1–4GlcNAc could arise from a small change in the orientation in the terminal Manα1–3 residue with respect to αGlcNAc and βGlcNAc.

When the Manα1–3 residue located on the 6-arm is substituted at its C2 position by αMan, the postulated hydrogen bond between the latter residue and the core GN is not possible. Thus, one would expect the conformational properties of such a structure to be significantly altered as compared to a high mannose structure with a terminal Manα1–3 residue on the 6-arm. Indeed, this effect is reflected in the ^{1}H NMR spectrum of the high mannose oligosaccharide containing nine mannoses (van Halbeek et al., 1980) where all the terminal residues in D3 have been substitued at their respective C2 by αMan. The α,β effect on the H1 resonance of the internal Manα1–3 residue of the 6-arm is now only 0.009 ppm, as compared to 0.060 ppm for the H1 resonance of the terminal Manα1–3 residue in D3. A second example is in the Man_6 isomer from IgM described by Cohen & Ballou (1980); in this compound the αMan1–2 residue is linked to the 6-arm 3t residue, thus preventing formation of the hydrogen bond. The result is that no splitting of the H1 resonance (~5.1 ppm) of 3t is observed in the spectrum of the oligosaccharide [Figure 8B of Cohen & Ballou (1980)].

With the linkage conformation for the Manα1–2Man unit set at (–50°, –20°) from previous studies (Brisson & Carver, 1983a), potential energy calculations on Manα1–2Manα1–3Manα1–6Manβ1–4GlcNAc predict that for $\omega = -60°$, the internal Manα1–3 residue can still come into close contact with the GlcNAc residue. Thus, if ω was restricted to –60°, the H1 resonance of the internal Manα1–3 should still experience a high anisotropic magnetic field (calculated shielding of –0.12 ppm) characterized by a large α,β effect. since, for $\omega = 180°$ no appreciable shielding is expected on the H1 resonance of the internal Manα1–3, the small α,β effect observed for a high mannose structure with an internal Manα1–3 residue on the 6-arm suggests that both rotamers ($\omega = -60°$ and $\omega = 180°$) are now in dynamic equilibrium, as in GGN.

Orientation of the 6-Arm in Bisected Hybrid Structures. Since in oligosaccharides of C3B and A3, which terminate in (α,β)GlcNAc, the $\alpha\beta$ effect on 3t H1 (0.05 ppm) is comparable to that in E3 and D3 (0.06 ppm) (Carver et al., 1981), and in the glycopeptides virtual coupling on the core GN H1 is still apparent (Brisson & Carver, 1982), the average orientation of the 6-arm must be similar for these compounds. Therefore, since the 3t H1 is in a region of high magnetic field anisotropy, the perturbations observed on the 3t H1 and the core GN H1 resonances (Table II), when the bis GN is present, are probably due to a slight reorientation of the 6-arm.

The effect of bis GN on the energetically available conformers was estimated from potential energy calculations on the structure Manα1–3Manα1–6(GlcNAcβ1–4)Manβ1–4GlcNAc with a bis GN linkage conformation of (60°, 10°) (Brisson & Carver, 1983a). For $\omega = -60°$, the minimum was the same as that found for high mannose structures containing a terminal Manα1–3 residue (3t) on the 6-arm, where a hydrogen bond between 3t O2-H and the carbonyl oxygen of the core GN was possible. However, the $\omega = 180°$ rotamer was also energetically probable. Despite this, the average orientation of the 6-arm was found to be the same as in high mannose structures.

On saturation of 6i H1 and 6t H1 in A3 (Figure 1e), NOE's are observed on the strongly coupled 4i H6–H6′ and on the strongly coupled 6i H5–H6 resonances. The computed enhancements for these NOE's using the linkage conformations deduced above for a bisected hybrid structure account for the observed NOE's (Table I). The large perturbations on the chemical shifts of the 4i H6 and 4i H6′ resonances (0.12 and –0.06 ppm, respectively), brought about by the presence of a bis GN in the structure, probably arise from the close proximity of the acetamido group of bis GN to the 4i hydroxymethyl group.

The orientation of the hydroxymethyl group on 4i is $\omega = -60°$ for bisected hybrid structures as compared to $\omega = 180°$ for bisected complex structures. This difference in ω explains the smaller chemical shift perturbation on the 4i H4 resonance in the former (0.11 ppm, C3B) than in the latter (0.31 ppm) (Table II), since the H4 resonance is no longer deshielded by O6 (Figure 2). Also, since bis GN H1 is close to 4i H4, by virtue of the linkage, a similar differential effect occurs for bis GN H1 in C3B (4.410 ppm) and in GGN(GN) (4.465 ppm).

Conclusion

In conclusion, nuclear magnetic resonance methods have been successfully applied to the determination of the three-dimensional structure of Asn-linked oligosaccharides in solution. The major conformational difference which exists between the various classes of glycopeptides is in the orientation and the flexibility of the α(1–6)-linked moiety. High mannose, hybrid, and bisected hybrid structures with a terminal Manα1–3 residue on the 6-arm have a well-defined stable solution conformation with the 6-arm folded back toward the core. In contrast, for biantennary complex type structures, the 6-arm can interconvert between two favorable rotamers about the C5–C6 bond of the internal Manα1–6 linkage. However, in the F_c portion of the crystal structure of a human IgG, which bears a complex biantennary structure, a unique orientation of the 6-arm was observed (Deisenhofer, 1981), which corresponded approximately to the solution structure with $\omega = -60°$. Thus, carbohydrate–protein interactions can stabilize a particular three-dimensional structure in a situation where more than one conformer is available in the isolated oligosaccharide. In bisected complex type structures, the bisecting GlcNAc stabilized the structure with the 6-arm folded back toward the core. However, the value of ω at the internal Manα1–6 linkage was now 180°, as opposed to a value of –60° in bisected hybrid, hybrid, and high mannose struc-

tures were the 6-arm is also folded back toward the core.

A knowledge of the three-dimensional structure of the carbohydrate chains of Asn-linked glycopeptides has brought to light many interesting features of their behavior in solution which in turn has led to a better appreciation of the molecular basis of the specificity in their biosynthesis (Brisson & Carver, 1983c).

Acknowledgments

We thank Harry Schachter, George Vella, Stephen D. Allen, and Saroja Narasimhan for the pure glycopeptides. Helpful discussions with Arthur Grey are acknowledged. We also thank Tom Lew for the incorporation of the graphics programs in our computer.

Registry No. GGN, 85995-13-7; GGN(GN), 86012-73-9; D3, 86012-74-0; A3, 86012-75-1; Manα1–3Manα1–6Manβ1–4GlcNAcβ, 85995-14-8; Manα1–6(Manα1–3)Manα1–OMe, 68601-74-1.

References

ApSimon, J. W., & Beierbeck, H. (1971) *Can. J. Chem. 49*, 1328–1333.

Brisson, J.-R., & Carver, J. P. (1982) *J. Biol. Chem. 257*, 11207–11209.

Brisson, J.-R., & Carver, J. P. (1983a) *Biochemistry* (preceding paper in this issue).

Brisson, J.-R., & Carver, J. P. (1983b) *Biochemistry 22*, 1362–1368.

Brisson, J.-R., & Carver, J. P. (1983c) *Can. J. Biochem.* (in press).

Carver, J. P., Grey, A. A., Winnik, F. M., Hakimi, J., Ceccarini, C., & Atkinson, P. H. (1981) *Biochemistry 20*, 6600–6606.

Cohen, R. E., & Ballou, C. E. (1980) *Biochemistry 19*, 4345–4358.

De Bruyn, A., & Anteunis, M. (1976) *Carbohydr. Res. 47*, 311–314.

Deisenhofer, J. (1981) *Biochemistry 20*, 2361–2369.

Gagnaire, D., Horton, D., & Taravel, F. R. (1973) *Carbohydr. Res. 27*, 363–372.

Longchambon, F., Ohanessian, J., & Gillier-Pandraud, H. (1981) *Acta Crystallogr., Sect. B B37*, 601–607.

Marchessault, R. H., & Perez, S. (1979) *Biopolymers 18*, 2369–2374.

Narasimhan, S. (1982) *J. Biol. Chem. 257*, 10235–10242.

van Halbeek, H., Dorland, L., Veldink, G. A., Vliegenthart, J. F. G., Michalski, J. C., Montreuil, J., Strecker, G., & Hull, W. E. (1980) *FEBS Lett. 121*, 65–70.

Warin, V., Baert, F., Fouret, R., Strecker, G., Spik, G., Fournet, B., & Montreuil, J. (1979) *Carbohydr. Res. 76*, 11–22.

Winnik, F. M., Carver, J. P., & Krepinsky, J. J. (1982) *J. Org. Chem. 47*, 2701–2707.

Quaternary Structure and Spin-State Transition in Azide Methemoglobin A†

Saburo Neya,* Sakae Hada, and Noriaki Funasaki

ABSTRACT: The temperature-dependent ultraviolet and visible absorption changes of human azide methemoglobin with and without inositol hexaphosphate (IHP) were examined in a 4–35 °C range. The 537-nm absorption change of IHP-free hemoglobin was about 1.2-fold larger than that of IHP-bound hemoglobin. The data were analyzed by considering the thermal spin equilibrium within the R and T conformers and the quaternary equilibrium between the two conformers. The spin equilibrium analysis suggested that the T conformer has a larger high-spin content than the R conformer. The quaternary equilibrium analysis, on the other hand, showed that the T conformer is more populated at lower temperature. The thermodynamic values for the quaternary equilibrium were determined to be $\Delta H = -13.3$ kcal/mol and $\Delta S = -47.6$ eu. The large negative ΔH and ΔS values were compensated for each other to give a small energy difference between the two quaternary states, e.g., $\Delta G_4 = 670$ cal/mol of tetramer at 20 °C. The coincidence of the temperature-dependent IHP-induced changes in the visible and ultraviolet absorptions of heme and aromatic chromophores at the subunit boundaries suggested that the quaternary transition energy is not localized at heme moiety. The reverse temperature dependence of the T conformer fraction as compared with the high-spin fraction of heme iron was interpreted as indicating that the appearance of the T state is not directly coupled with an increase in the strain of Fe–N(F8 His) linkage in azide methemoglobin A.

The increased ligand affinity of oxyhemoglobin relative to deoxyhemoglobin lies in a structural difference between the relaxed (R) and tense (T) quaternary states. The X-ray analyses on the liganded (Ladner et al., 1977) and unliganded (Fermi, 1975) hemoglobins suggested that the iron displacement from the heme plane, linked to the spin state of heme iron, could act as a switch in the quaternary structure (Perutz, 1970). The quaternary structure and spin-state relationship were applied to methemoglobin complexes (Perutz et al., 1974a,b, 1978). On the basis of ligand binding, spectroscopic, and X-ray results, it was found that an allosteric effector IHP[1] is capable of converting high-spin methemoglobin from the R to T states (Fermi & Perutz, 1977; Perutz, 1979). The low-spin methemoglobin exhibited much weaker IHP-induced responses, which were not regarded as to be associated with the quaternary transition. It was, however, found that IHP can promote a substantial conversion of low-spin methemoglobin to the T state (Neya & Morishima, 1981a). The presence of the T state in low-spin methemoglobin seems to be inconsistent with the simple coupling between the position of heme iron and the globin quaternary structure.

To provide an insight into the influence of iron spin state on the globin quaternary structure and to examine the dynamic

† From the Department of Physical Chemistry, Kyoto College of Pharmacy, Yamashina, Kyoto 607, Japan. *Received January 26, 1983.* This work was supported by a grant-in-aid for Scientific Research from the Ministry of Education, Science and Culture, Japan.

[1] Abbreviations: IHP, inositol hexaphosphate; Pipes, 1,4-piperazinediethanesulfonic acid.

0006-2960/83/0422-3686$01.50/0